DIRECT-S WAVE MODES PRODUCED BY VERTICAL AND HORIZONTAL VIBRATORS

ENGIN ALKAN and BOB HARDAGE

Exploration Geophysics Laboratory, Bureau of Economic Geology, Austin, TX 78713-8924, U.S.A.

(Received August 7, 2012; revised version accepted February 15, 2013)

ABSTRACT

Alkan, E. and Hardage, B.A., 2013. Direct-S wave modes produced by vertical and horizontal vibrators. *Journal of Seismic Exploration*, 22: 147-168.

Horizontal vibrators are considered to be the optimal source for generating direct-S modes, which are S modes produced directly at a source station, not by mode conversion at interfaces remote from a source station. We show some results of a field test in which we investigated direct-S modes produced by vertical-force seismic sources. The test data were acquired by positioning horizontal vibrators and various vertical-force sources (vertical vibrator, vertical impact, shot-hole explosive) at the same source stations and recording their downgoing illuminating wavefields with a vertical array of 3-component geophones. In this paper, we compare only direct-S modes produced by vertical vibrators and horizontal vibrators. We show that there are strong similarities between the direct-S modes produced by these two sources. This investigation has considerable economic value because if it can be established that direct-S modes produced by vertical-force sources can be substituted for direct-S modes produced by horizontal vibrators, a large number of direct-S sources become available that can be used in any environment where P-wave seismic data are acquired.

KEY WORDS: direct-S, vertical force source, horizontal vibrator, vertical vibrator, P- and S-radiation.

INTRODUCTION

We present here an investigation of direct-S radiation patterns generated by vertical and horizontal vibrators. In our terminology, a direct-S mode is an S wave produced directly at the point where a seismic source applies its force vector to the earth. We describe our field-test procedure and then analyze VSP data that describe downgoing direct-S wavefields generated by two types of vibratory seismic sources-a vertical vibrator that applies a vertical force to the

0963-0651/13/$5.00

earth, and a horizontal vibrator that applies a horizontal force to the earth. In the analyses presented here, we demonstrate that strong direct-S modes are produced by vertical vibrators and that these vertical-vibrator direct-S modes are reasonably equivalent to direct-S modes produced by horizontal vibrators, the latter being the sources most geophysicists prefer to use to generate direct-S modes.

At our test site, we found that the highest frequency in a direct-S mode was 50 to 55 percent of the highest frequency component of the vibrator sweep that generated the mode. Because vertical vibrators can be swept to higher frequencies than horizontal vibrators, direct-S modes produced by vertical vibrators have wider frequency spectra. Thus vertical-vibrator direct-S wavelets should provide better spatial resolution of geologic targets than do direct-S modes produced by horizontal vibrators.

DEVINE TEST SITE

This field test was done at the Devine Test Site operated by the Bureau of Economic Geology, a research unit of The University of Texas at Austin. The Devine Test Site was constructed by Sohio southwest of San Antonio, Texas, near the town of Devine (Fig. 1a), in the 1980's when Sohio was developing crosswell seismic and electromagnetic profiling technologies. After Sohio and BP merged, BP transferred the test site to The University of Texas at Austin so that the property could be managed by the University as a public test site. An aerial photo showing the distribution of test wells across the property is included as Fig. 1b.

The stratigraphy penetrated by the test wells is labeled on the well log curves displayed as Fig. 2. These logs were recorded in well 4 (Fig. 1b) and define V_P and V_S velocities and gamma-ray readings across the rock units that form the seismic propagation medium beneath the test-site property. These log measurements start immediately below the base of surface casing, which is at a depth of 532 ft (162 m) in well 4 where these logs were recorded.

SOURCE-RECEIVER GEOMETRY

The source-receiver geometry we utilized to evaluate surface-source P- and S-radiation patterns combined the concepts of horizontal wave testing (involving only a horizontal receiver array) and vertical wave testing (involving only a vertical receiver array) as described by Hardage (2009, 2010). Much of our wave-test philosophy was inspired by the field technique published by Robertson and Corrigan (1983), who used a single subsurface 3C geophone to quantify SH- and SV-radiation patterns produced by a horizontal vibrator.

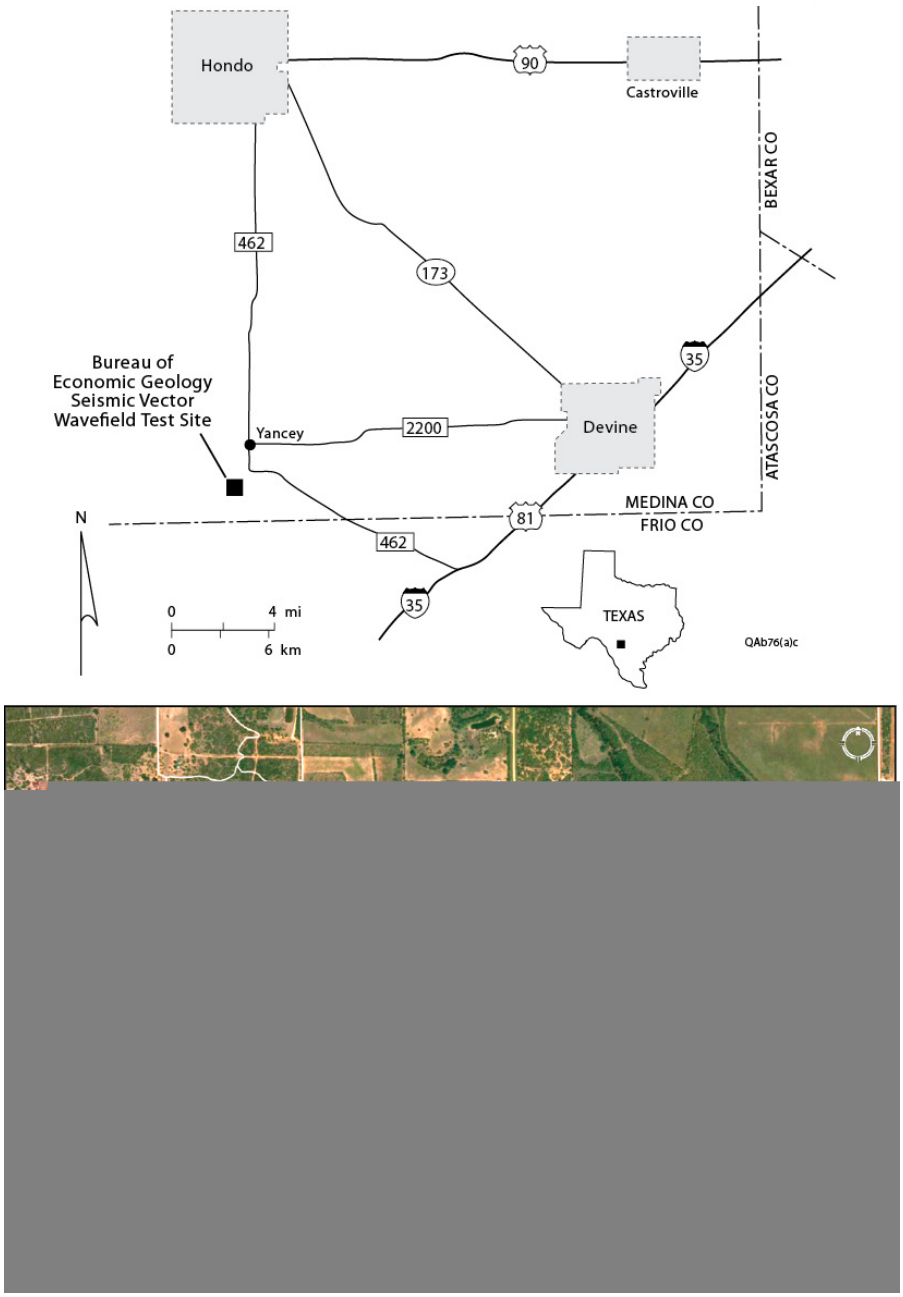

Fig. 1. (a) Location of the 100-acre Devine Test Site in Medina County, Texas. The city of San Antonio is approximately 50 km east of the town of Hondo shown on this map. (b) Photo showing the positions of test wells 4, 2, and 9 across the test-site property. These wells were constructed for the purpose of deploying downhole instrumentation, particularly seismic sources and receivers and logging tools. All wells are 3000 ft (914 m) deep.

We expanded their methodology by using a vertical array of 24 3C geophones, deploying vertical-force, inclined-force, and horizontal-force sources, and analyzing P-wave radiation patterns produced by these sources in addition to S-wave radiation patterns. Although we generated a comprehensive source-test database, only analyses of direct-S waves produced by vertical and horizontal vibrators and recorded by a downhole vertical array of receivers will be presented in this paper.

Well 4 on the Devine Test Site property was chosen for the location of the vertical receiver array. A 24-station receiver system was deployed in this well (Fig. 3). Receiver stations spanned a depth interval extending from 500 to 1632 ft (152.4 to 497.4 m). The velocity layering and lithology variations local to this vertical sensor array are defined by the log character inside the shaded interval shown on Fig. 2.

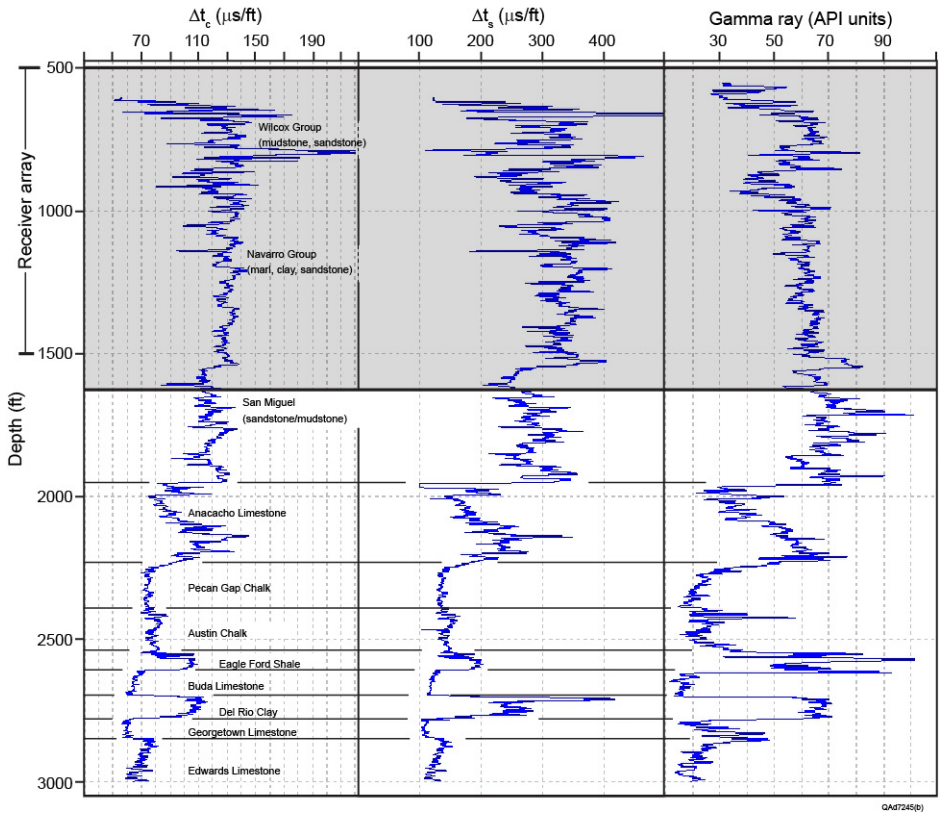

Fig. 2. V_P and V_S velocity logs and gamma-ray log acquired in well 4 on the Devine Test Site. The shaded interval defines the depth range over which downhole geophones were deployed for the source tests described here.

In this source test, we defined the inline (radial) direction as the azimuth of the straight-line profile that passed through the nine inline surface-source stations and the receiver well (Fig. 3). The crossline (transverse) direction was perpendicular to the vertical plane of this profile. At inline source stations 3 and 5 (offset 500 ft (152.4 m) and 1000 ft (304.8 m)) from the receiver well), a horizontal vibrator was positioned at several azimuth orientations to generate data describing the azimuth-dependent character of S-wave radiation patterns produced by a horizontal-vibrator source. The azimuth directions in which each horizontal force was applied to the earth surface at these two offset stations are illustrated on Fig. 4. This diagram describes how the horizontal vibrator was positioned in 10° azimuth increments to transition from a crossline baseplate orientation (0° azimuth of vehicle headlights in our notation on Fig. 4) to an inline baseplate orientation (90° azimuth of vehicle headlights). In this diagram, line AB is the inline (radial) direction. A photo of a horizontal vibrator generating azimuth-dependent data at source station 3 is shown as Fig. 5.

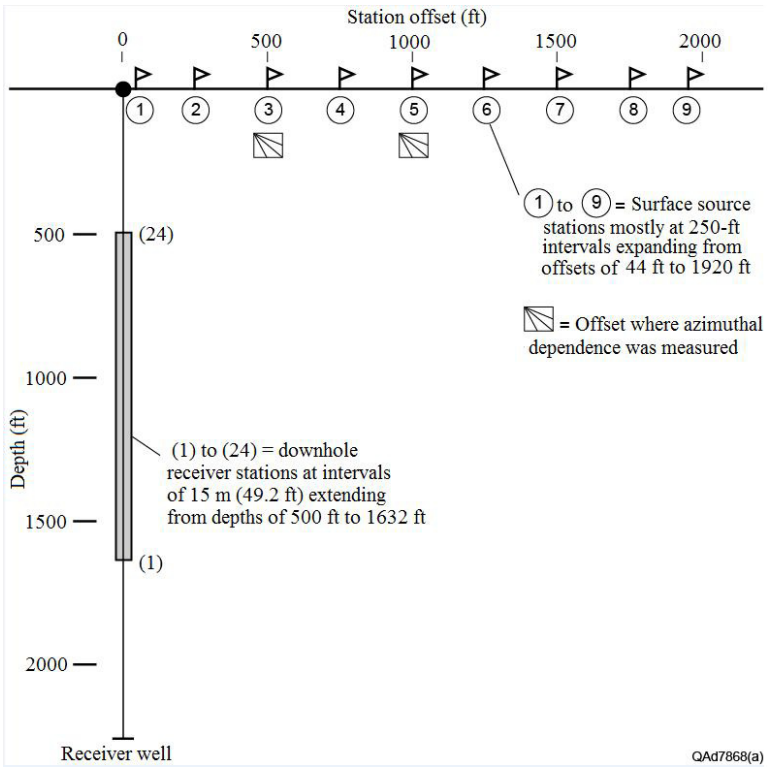

Fig. 3. Source-receiver geometry used to analyze P and S radiation patterns emitted by surface-based seismic sources. A 24-station vertical array of 3C geophones spaced at intervals of 15 m (49.2 ft) spanned the depth interval from 500 to 1632 ft (152.4 to 497.4 m) in well 4. Source stations were offset from the test well at intervals of 250 ft (76 m). Horizontal-force sources were activated at several different azimuth orientations at source stations 3 and 5, as shown by the special labels at these stations.

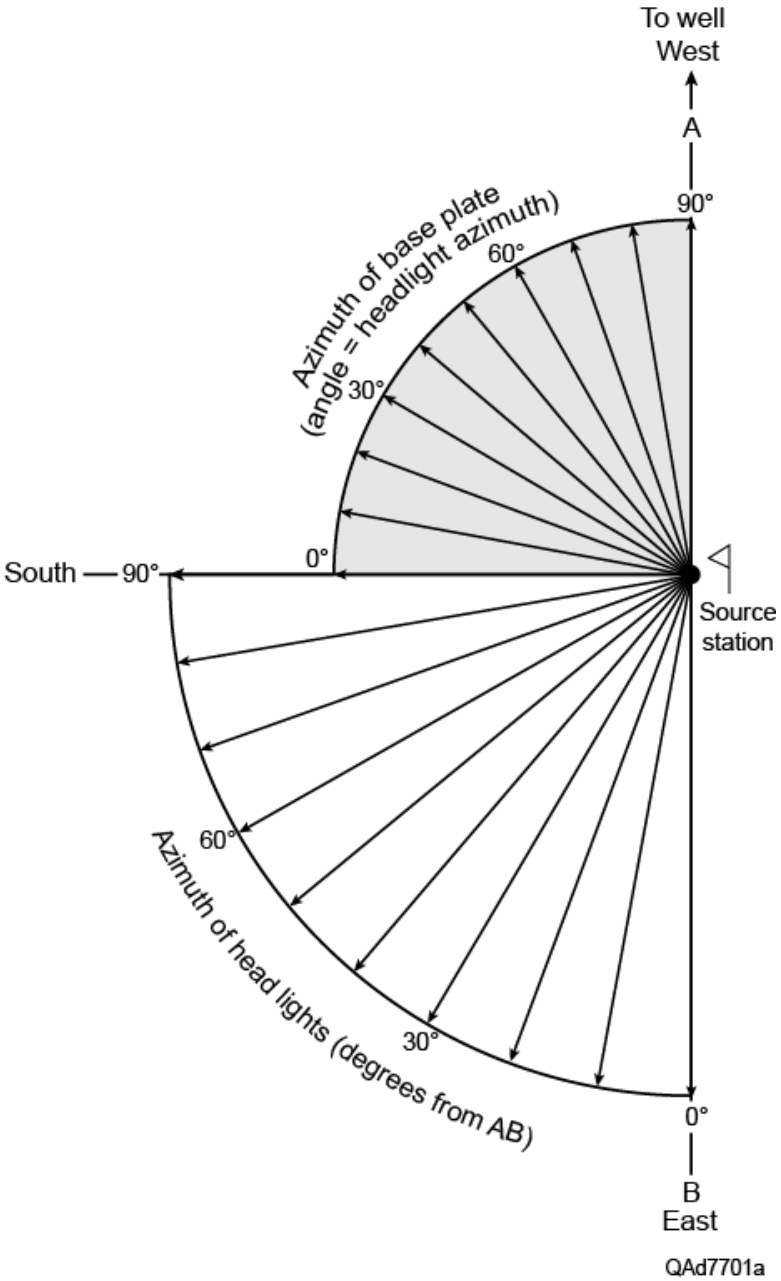

Fig. 4. Map view of azimuth directions in which horizontal forces were applied at source stations 3 and 5. The diagram is drawn to describe the azimuth positions assumed by a horizontal vibrator (bottom) and its base plate (top).

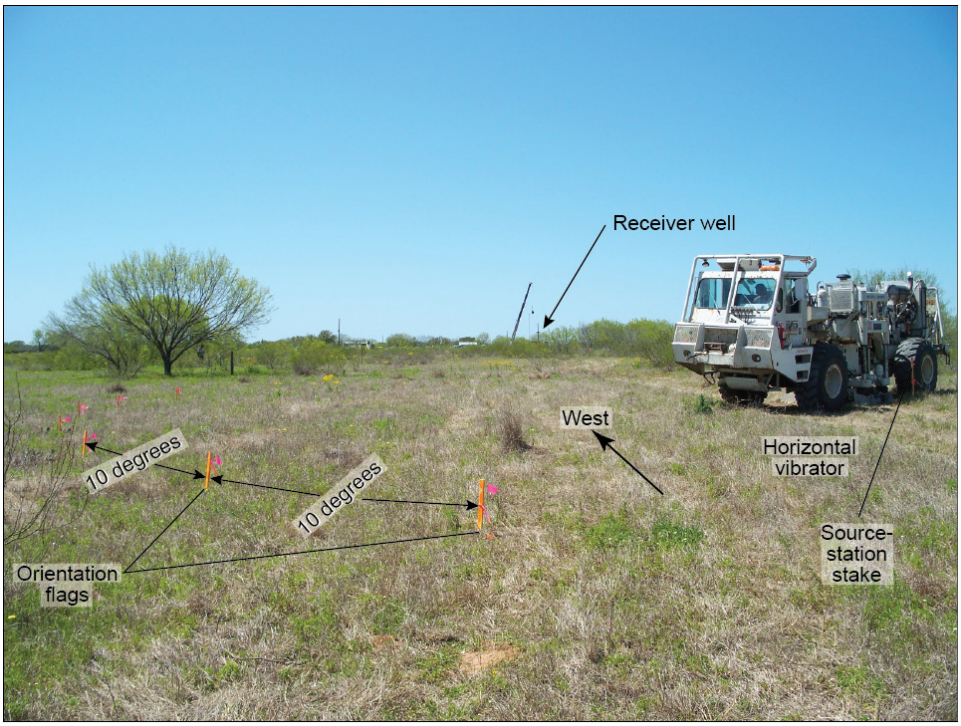

Fig. 5. Horizontal vibrator executing a sequence of 10° azimuth positions at source station 3.

VERTICAL-FORCE SOURCES AND DIRECT-S MODES

A robust amount of SV shear energy is produced by a vertical-force seismic source. This principle is illustrated on Fig. 6 which shows the geometrical shapes and relative strengths of P and SV energy propagating away from the point where a vertical-force source applies its force vector to a homogeneous earth. The P- and SV-radiation patterns shown by this figure are replications of analyses published by Miller and Pursey (1954) and White (1983). Both P- and SV-modes are generated directly at the point where vertical force vector F contacts the earth's surface. The relative strengths of P and SV modes propagating at any take-off angle from the source station are indicated by the radial distances from the origin point to the outer edges of the P and SV radiation patterns. For example, in Fig. 6a the magnitude of the SV mode propagating at an angle of 30-degrees from vertical is approximately 8 times greater than the magnitude of the P-mode propagating in that same take-off direction.

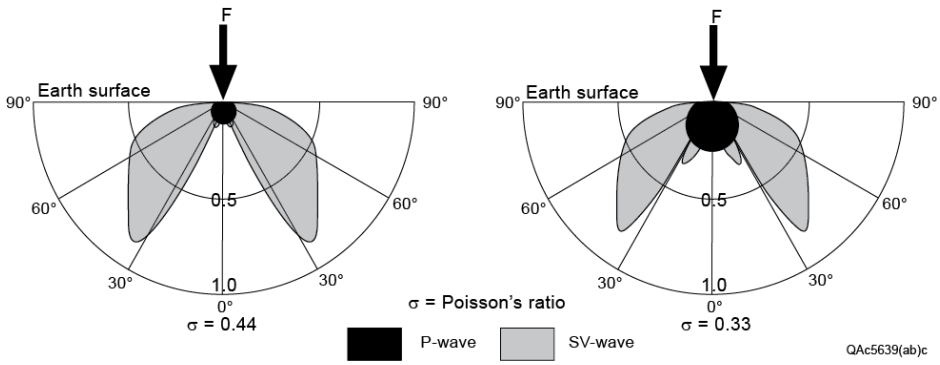

Fig. 6. P- and SV-radiation patterns produced when a vertical force is applied to the surface of a homogeneous earth. (a) A soft earth surface. (b) A hard earth surface. In both cases more SV-energy radiates from the source station than does P-energy.

Previous researchers have used this model as the starting point for investigations into direct-S illumination of geologic targets by vertical-force sources. Edelmann (1981) analyzed S-displacement vectors associated with raypaths slanted at arbitrary takeoff angles in the SV lobes of Fig. 6 to conclude that a vertical vibrator should create SH illumination in addition to SV-illumination. Fertig and Krajewski (1989) used the same radiation diagram in their study and made the important declaration that not only does a vertical vibrator produce direct-S modes, but so does a shot-hole explosive and an air gun in a pit. Lynn and McCardle (1990) also state direct-S waves are produced by air guns operating in rectangular pits and show direct-S modes labeled as SV and SH produced by vertical vibrators.

The radiation of direct-S modes from shot-hole explosives has been documented by Wright and Carpenter (1962) following investigations to determine how to detect tests of buried nuclear devices. They made plaster casts of shot-hole cavities that showed asymmetric deformation generated by explosive detonations. They state that "on no occasion has an underground firing failed to give rise to significant transverse seismic waves". Fertig (1984) also concludes a shot-hole explosive generates direct-S modes but associates the generation of these modes to P-to-SV conversion at the earth-air interface above a shot. Zhou et al. (2005) show VSP data in which they propose azimuthal anisotropy local to a source station as being the reason they observe both direct SH and qSV modes propagating away from vertical-vibrator stations. Yang et al. (2007) present excellent data examples of direct-S modes produced by both vertical vibrators and shot-hole explosives and refer to pure-S (SH) modes radiating from these vertical-force sources in addition to SV modes.

We emphasize the P- and SV-radiation patterns on Fig. 6 apply for wave propagation in a homogeneous elastic half space. When azimuthal anisotropy exists in shallow earth layers, wave propagation needs to be described in terms of natural coordinate axes. Others have analyzed VSP data acquired at the Devine Test Site where our data originate and concluded a weak S-wave anisotropy is present in the local rock layering. Raikes (1991) used an inclined-impact source to produce horizontal-force source VSP data and concluded S-wave anisotropy was less than 3-percent across the property. She found a time delay of 12 ms between fast and slow modes at geophone depths of 900 m, and estimated cracks were oriented at an azimuth of 10 degrees from North. The same data were later studied by Li et al. (1998) who confirmed S-wave anisotropy was less than 3-percent, found fast and slow modes travel times differed by 10 ms at deep (900 m) receiver stations, and estimated one natural coordinate axis was oriented 60 degrees from North.

The important distinction between our study and all of these that are cited is that none of the above studies used a combination of vertical-force and horizontal-force sources in the same test so direct-S modes produced by both sources types could be directly compared. Our approach has been to deploy vertical vibrators and horizontal vibrators at the same surface coordinates and to record downgoing direct-S modes generated by these sources with the same vertical receiver array. We do not delve into the effects of azimuthal anisotropy on P- and SV-radiation in the data analyses we show. We describe only a straight-forward field experiment in which we positioned a vertical vibrator and a horizontal vibrator at the same source station and recorded the direct-S wavefields produced by each vibrator with a vertical array of downhole 3C geophones. We ignore the issue of whether the downgoing direct-S wavefields do or do not propagate in an azimuthally anisotropic medium and simply compare the character of the direct-S wavefields recorded by radial geophones and transverse geophones for each type of vibrator source. The end result is that we observe a strong similarity between direct-S modes produced by vertical and horizontal vibrators at the Devine Test Site.

TRANSFORMING VSP TEST DATA TO WAVE-MODE DATA

In a vertical receiver well, azimuth orientations of X,Y horizontal geophones differ at each downhole station because sensor packages are deployed on twisted-wire cable that rotates as it spools off a cable reel. As a result, sensors rotate by different amounts when they reach different deployment depths. Phase shifts and amplitude variations introduced into horizontal-sensor data by station-to-station variations in receiver orientation do not allow individual events or distinct wave modes to be recognized, particularly S-wave events that dominate horizontal-sensor response. Receivers must be

mathematically oriented to consistent azimuths and to proper inclinations to define downgoing and upgoing P- and S-modes.

Transformations of borehole receivers from in situ X, Y, Z orientations to a data space where receivers are oriented to emphasize P, radial-shear (SR), and transverse-shear (ST) events have been practiced in VSP technology for several decades (DiSiena et al., 1981; Hardage, 2000). A graphical description of the transformation of receivers from X, Y, Z data space to P, SR, ST data space is shown on Fig. 7. In this approach, the downgoing P-wave first arrival is analyzed at each receiver station to determine azimuth rotation angle θ and inclination angle ϕ such that when the 3C sensors are rotated by these angles, one sensor is aligned with the downgoing P-wave displacement vector oriented along raypath RS. A second sensor is then aligned with radial-S displacement vector SR, which is assumed to be orthogonal to RS and to be in vertical plane ROS. The third sensor is aligned with the transverse-S displacement vector ST, which is assumed to be orthogonal to plane ROS.

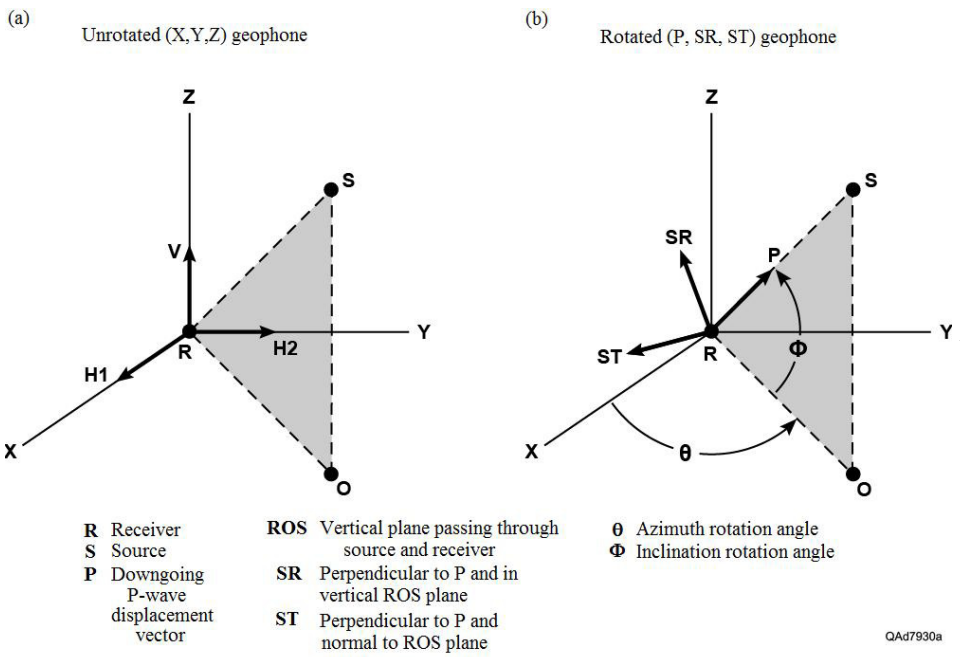

Fig. 7. Transformation of X, Y, Z receivers to P, SR, and ST receivers. (a) Orientation of 3C geophone as deployed in X,Y,Z data-acquisition space. (b) Mathematical orientation of 3C geophone to align sensor elements with displacement vectors associated with downgoing P, SR, and ST wave modes.

WAVEFIELD SEPARATION

In our analysis, we examine multicomponent data generated by vertical and horizontal vibrators using all sensor components of the 3C geophones that were deployed as a downhole receiver array. Fig. 8 illustrates downgoing illuminating VSP wavefields produced by vertical, inline-horizontal, and crossline-horizontal vibrators after downhole geophones have been rotated in azimuth and then in inclination to align sensors as illustrated on Fig. 7. Visual inspection of the data on Fig. 8 shows there is an undesirable amount of high-amplitude reverberation and wavelet distortion in the data recorded by the top-most 5 or 6 receiver stations. The logs on Fig. 2 indicate there is significant variation in stratigraphic layering in this interval of the receiver well. The variations in layer velocities above 800 ft (243.8 m) cause some events to undergo critical refraction. We considered deleting the data above 800 ft (243.8 m) but decided to leave the data in our graphic displays to maintain completeness of data information. Below a receiver station depth of 800 ft (243.8 m), S-event waveshapes are stable and direct-S modes produced by vertical and horizontal vibrators have essentially the same arrival times at each downhole receiver station. However, visual examination shows the range of frequencies recorded on radial and transverse component sensors are different for vertical and horizontal vibrators.

It is important to recognize the differences in radial-S and transverse-S wavefields produced by the vertical vibrator. The radial-S component of the vertical-vibrator direct-S mode (Fig. 8d) shows a prominent downgoing P-SV event generated at a time coordinate of approximately 250 ms not far below a depth of 500 ft (152 m). In contrast, the transverse-S component (Fig. 8g) shows no evidence of P-SV converted events. We have not observed converted-shear events on any transverse-S data produced by the several vertical-force source data sets we have examined.

COMPARING FREQUENCY CONTENT OF DIRECT-S MODES

Prudent field practice is to limit the highest frequency of a horizontal-vibrator sweep to approximately 50 Hz. Horizontal vibrators can sweep to frequencies higher than 50 Hz, but tend to have an unacceptable number of mechanical problems when forced to operate at high frequencies because of undue stress on hydraulic systems and structural supports. It is also challenging to maintain proper phase locking of horizontal vibrators at high frequencies. For these reasons, the sweep range of the horizontal vibrators used in our field tests was constrained to a bandwidth of 4 to 50 Hz, which is a common sweep range people use when deploying horizontal vibrators in exploration programs. In contrast, vertical vibrators can sweep to frequencies well above 100 Hz without undue mechanical problems or phase-locking issues.

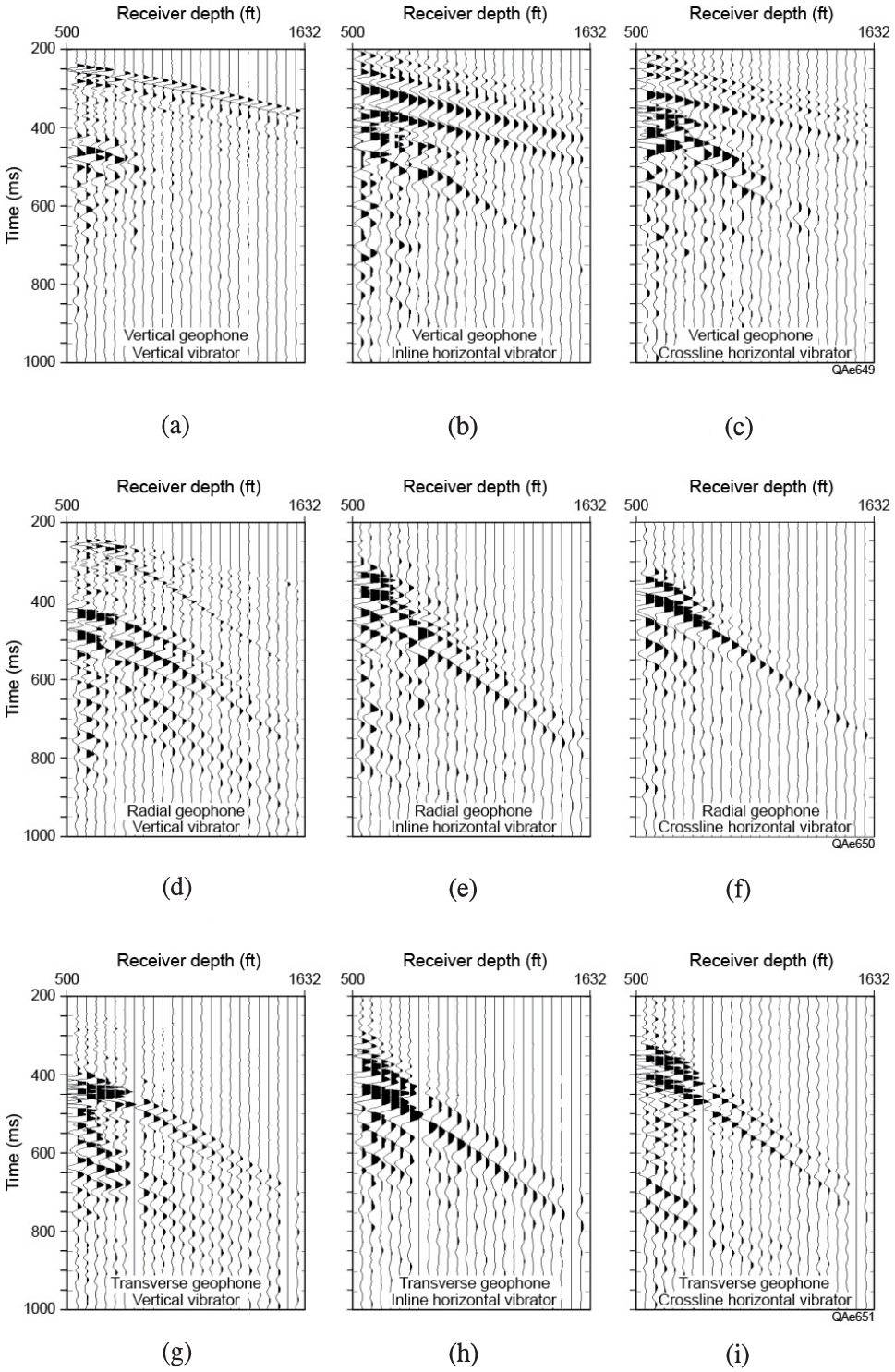

In our field experiment, the sweep range of the vertical vibrators was set at a modest interval of 8 to 96 Hz. When utilizing vertical and horizontal vibrators in data-acquisition projects, it is common practice to set sweep parameters so that the start and stop frequencies and frequency bandwidths used for vertical vibrators are a factor of 2 greater than the equivalent sweep parameters used for horizontal vibrators. We followed this common field practice in our field tests.

Quantifications of the differences in frequency content of direct-S modes produced by vertical-force and horizontal-force vibrators are illustrated on Figs. 9 and 10. The radial component of the direct-S mode generated by a vertical vibrator is compared with the radial component of the direct-S mode produced by a horizontal vibrator on Fig. 9; the transverse components of direct-S modes radiating from these two vibratory sources are compared on Fig. 10. Some important wave physics principles are exhibited by these data:

1. For both vertical and horizontal vibrators, the highest frequency in the propagating direct-S wavelet observed at our test-site was 50 percent to 55 percent of the highest frequency used in the vibrator sweep. For example, a 50-Hz upper sweep limit for the horizontal vibrator resulted in an upper frequency of approximately 28 Hz in the downgoing direct-S wavelet for that source, and a 96-Hz upper sweep limit for the vertical vibrator created an upper frequency of 50 to 55 Hz in the direct-S illuminating wavelet for that vertical-force source.
2. In terms of octaves, the bandwidths of direct-S wavelets propagating from both horizontal and vertical vibrators are approximately the same, with wavelets from each source spanning slightly less than three octaves (4 to 28 Hz for the horizontal vibrator, and 8 to 55 Hz for the vertical vibrator).
3. Because the bandwidth of the direct-S wavelet generated by a vertical vibrator spans higher frequencies than does the bandwidth of the direct-S wavelet produced by a horizontal vibrator, a vertical vibrator should provide better S-wave resolution of geologic targets than can a horizontal vibrator.

Item 3 of this list is particularly important and may result in wider use of vertical-force-source direct-S wavefields in future seismic evaluations of prospect areas.

Fig. 8. Comparison of multicomponent data recorded by vertical (a,b,c), radial (d,e,f), and transverse (g,h,i) sensors after rotation of the downhole 3C VSP geophones as defined on Fig. 7. These wavefields were generated by vertical (a,d,g), inline-horizontal (b,e,h), and crossline-horizontal (c,f,i) vibrators positioned at the same source station. The orientations and couplings of the downhole receivers were not altered during the data recording. Data recorded at receiver stations above 800 ft (243.8 m) are distorted by critical refractions and interbed reverberations.

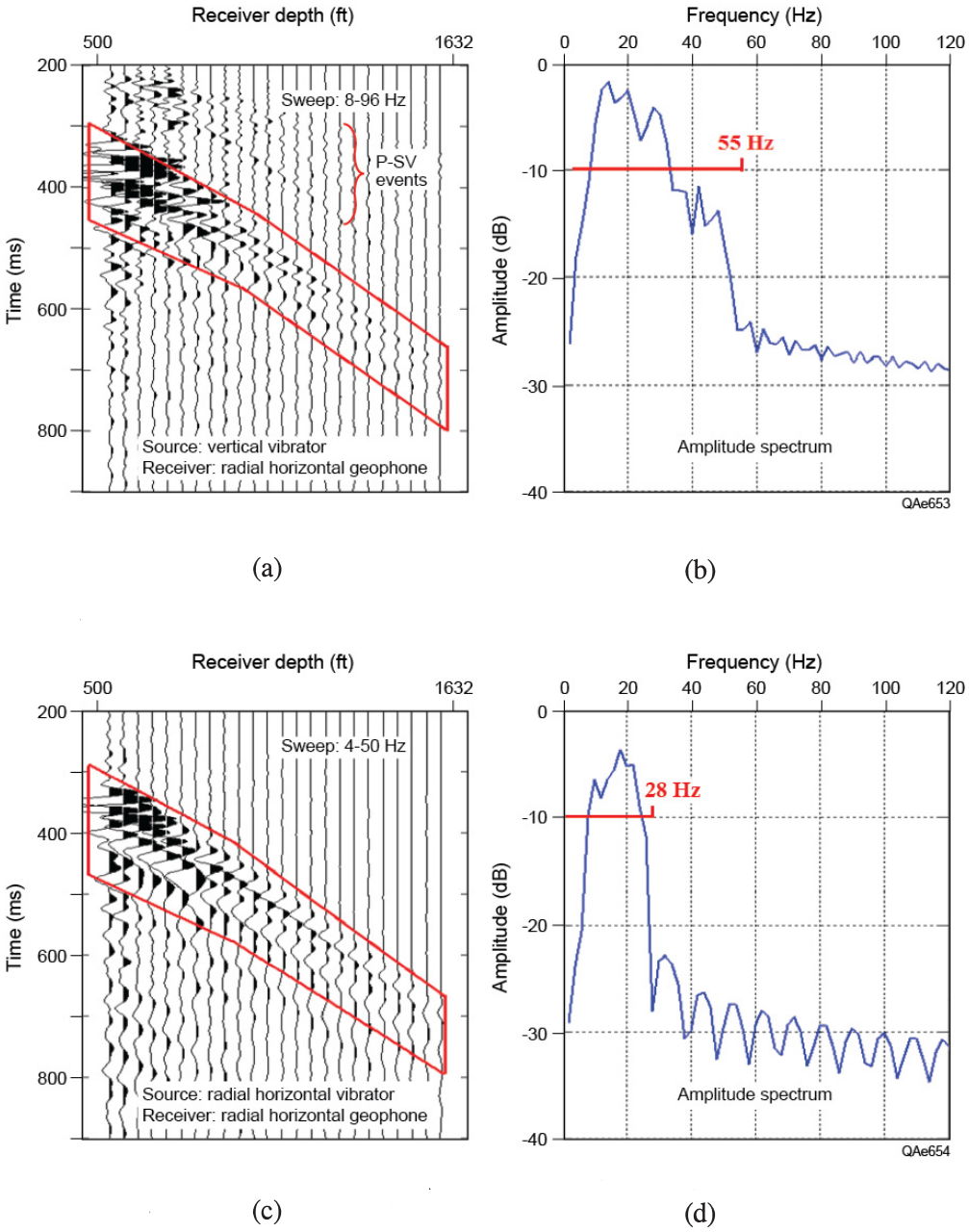

Fig. 9. Comparison of radial-S data generated by (a) a vertical vibrator and (c) an inline horizontal vibrator positioned at the same source station. Data were recorded by the same vertical array without altering receiver orientations or couplings. The amplitude spectrum of these direct-S wavefields are shown as (b) and (d). Data recorded at receiver stations above 800 ft (243.8 m) are distorted by critical refractions and interbed reverberations.

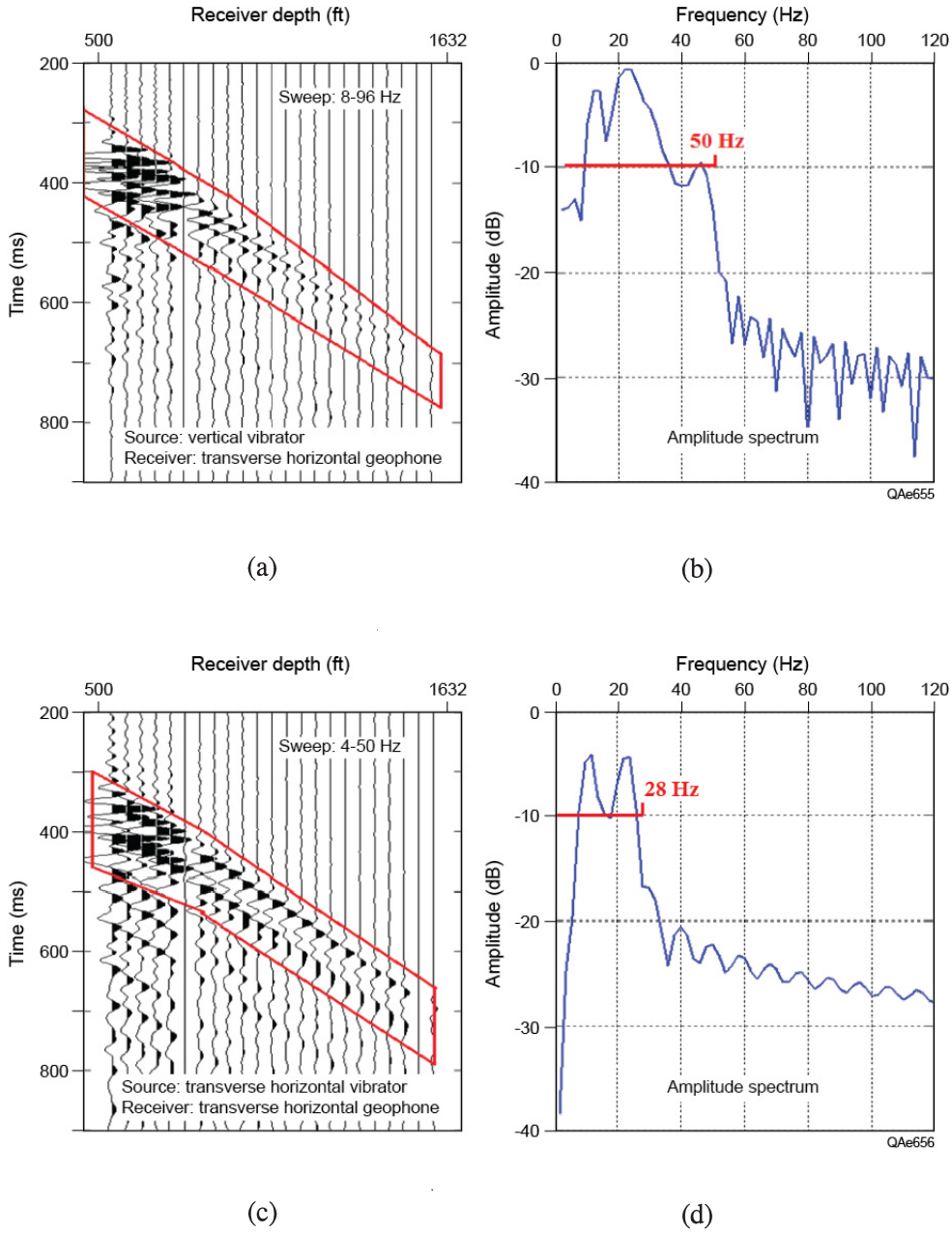

Fig. 10. Comparison of transverse-S data generated by (a) a vertical vibrator and (c) a crossline horizontal vibrator positioned at the same surface station. Data were recorded by the same vertical array without altering receiver orientations or couplings. The amplitude spectrum of each direct-S illuminating wavelet is shown as (b) and (d). Data recorded at receiver stations above 800 ft (243.8 m) are distorted by critical refractions and interbed reverberations.

(a)

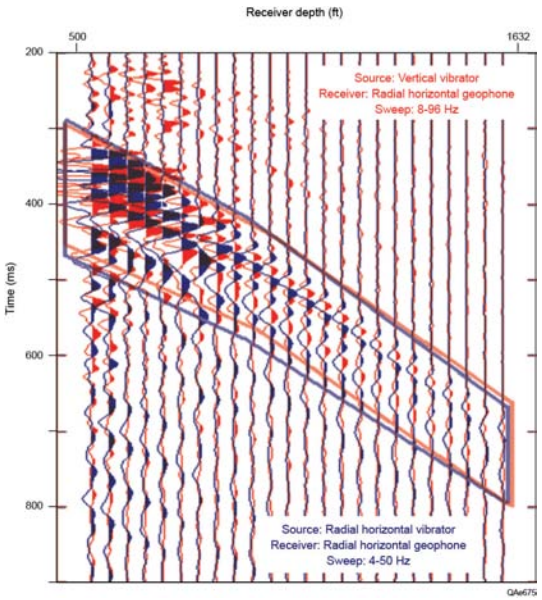

(b)

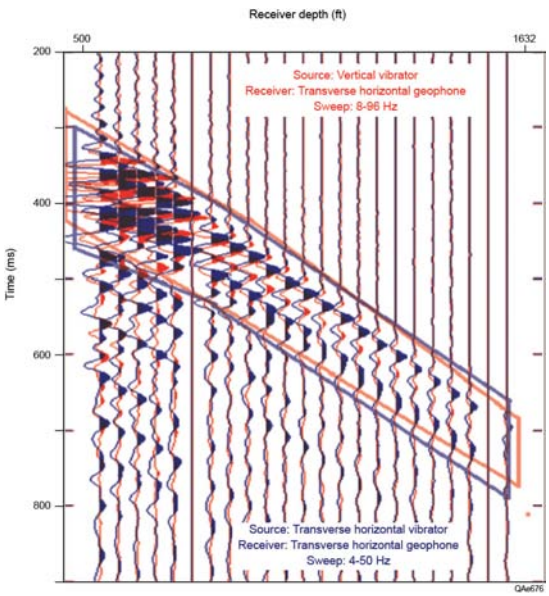

Fig. 11. (a) Radial direct-S wavefield produced by a vertical vibrator (red traces) overlain by the radial direct-S wavefield produced by a radial horizontal vibrator (blue traces). (b) Transverse direct-S wavefield produced by a vertical vibrator (red traces) overlain by the transverse direct-S wavefield produced by a transverse horizontal vibrator (blue traces). Vibrators were positioned at the same surface source station. Data were recorded by the same vertical array without altering receiver orientations or couplings. Data recorded at receiver stations above 800 ft (243.8 m) are distorted by critical refractions and interbed reverberations.

We illustrate the similarity between direct-S modes produced by horizontal vibrators and vertical vibrators by overlaying the downgoing direct-S modes produced by each source so the arrival times and wavelet attributes of the modes can be more easily compared. These wavefield comparisons are displayed on Fig. 11. The direct-S radial wavefield propagating from the horizontal vibrator (Fig. 11a) has a polarity opposite to that of the radial direct-S mode produced by the vertical vibrator because the horizontal vibrator was oriented North, causing the first motion of its baseplate (the direction of its radial-S polarity) to be away from the receiver well (Fig. 4). In contrast, the radial-S vector produced by the vertical vibrator was oriented toward the receiver well. Rather than reverse the polarity of one of the wavefields displayed on Fig. 11a, we left them as shown because this dual-color display of opposite-polarity data helps some people better judge the equivalence of the two modes for undistorted data recorded by receivers below 800 ft (243.8 m). The polarities of the transverse component of the vertical-vibrator and horizontal-vibrator direct-S wavefields are identical (Fig. b) and are essentially exact copies of each other when data above 800 ft (243.8 m) are ignored.

The comments above focus only on data within the outlined windows on each display, which define the downgoing direct-S modes produced by each vibrator. When data character outside these direct-S data windows are considered, there are several downgoing P-to-S converted events in the vertical vibrator data that are absent in the horizontal-vibrator data. The most obvious downgoing converted-SV mode is the event that originates near a depth of 500 ft (152 m) that precedes the direct-S data window (Fig. 11a). These downgoing converted-S events contribute noise in radial-S data produced by a vertical vibrator that does not have to be dealt with when a horizontal vibrator is used. No downgoing converted modes exist in transverse-S data produced by a vertical vibrator (Fig. 11b).

Visual examination of both of these dual-wavefield displays causes us to conclude that at this test site, except for the different frequency bandwidths documented on Figs. 9 and 10, the downgoing direct-S wavefields produced by a vertical vibrator are reasonably equivalent to the downgoing direct-S modes produced by a horizontal vibrator. We plan to continue field tests to confirm if there are geologic conditions where direct-S modes produced by vertical vibrators strongly differ from direct-S modes produced by horizontal vibrators. The close equivalence of direct-S wavefields produced by vertical and horizontal vibrators is an important principle that has not to our knowledge been documented in geophysical literature.

We close this analysis of vibrator-generated direct-S modes by presenting data that illustrate map views of the radial-S and transverse-S radiation lobes that propagated away from the horizontal-vibrator source we positioned at source station 3 (Fig. 3). An equivalent analysis has been published by

Robertson and Corrigan (1983), and we wished to repeat their analysis procedure because our test data were collected over a different type of earth surface than what existed at the site used by these earlier investigators, and our wavefields propagated through a geologic section that had a higher degree of stratigraphic layering. As shown on Fig. 3, we deployed a horizontal vibrator at source stations 3 and 5 so that its base plate was positioned at azimuths ranging from 0° to 90° relative to inline profile AB passing through source and receiver stations (Figs. 4 and 5). Data recorded by the downhole vertical array of 3C geophones could then be analyzed in the manner used by Robertson and Corrigan (1983). Our results are presented as Fig. 12; the corresponding radial-S and transverse-S radiation patterns published by Robertson and Corrigan (1983) are shown on Fig. 13 for comparison.

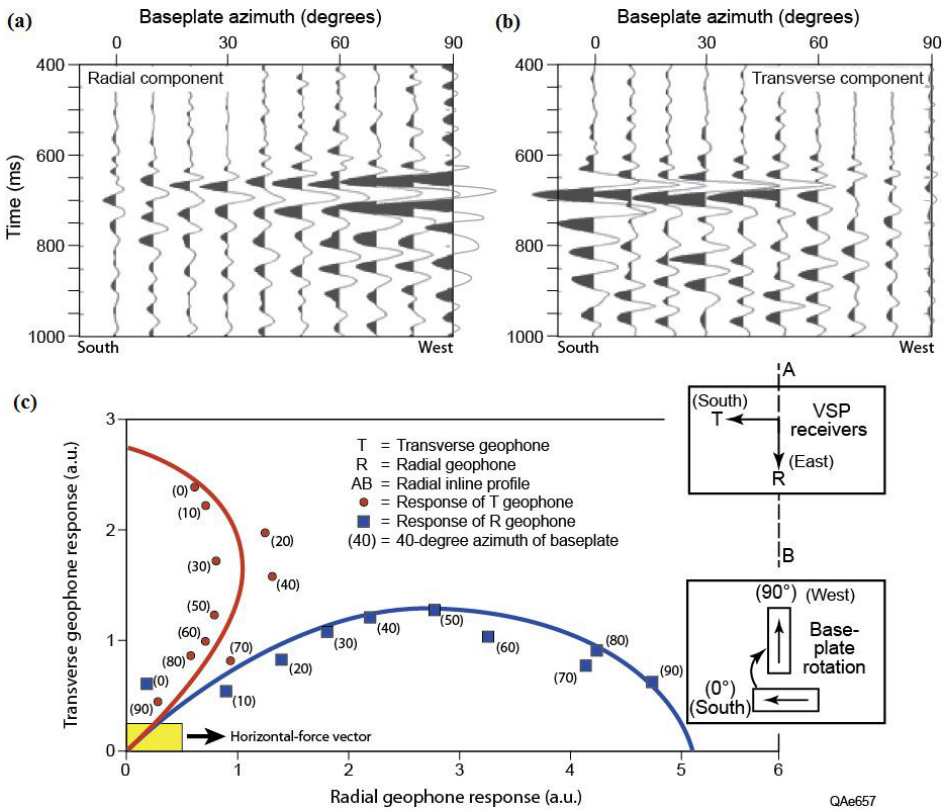

Fig. 12. (a) Azimuth-dependent radial-S data produced by a horizontal vibrator oriented in azimuth increments of 10° at source station 3 (Fig. 3). (b) Azimuth-dependent transverse-S data produced by the same horizontal vibrator.The sequential azimuth orientations of the vibrator base plate is described on Figs. 4 and 5. The receiver was positioned at downhole station 19 at a depth of 1386 ft (422 m) as shown in Figs. 2 and 3. (c) A map view of radial-S and transverse-S amplitude strengths from (a) and (b) showing the geometrical spreading of radial-S (solid square data points) and transverse-S (solid circle data points) modes from the horizontal-force source station.

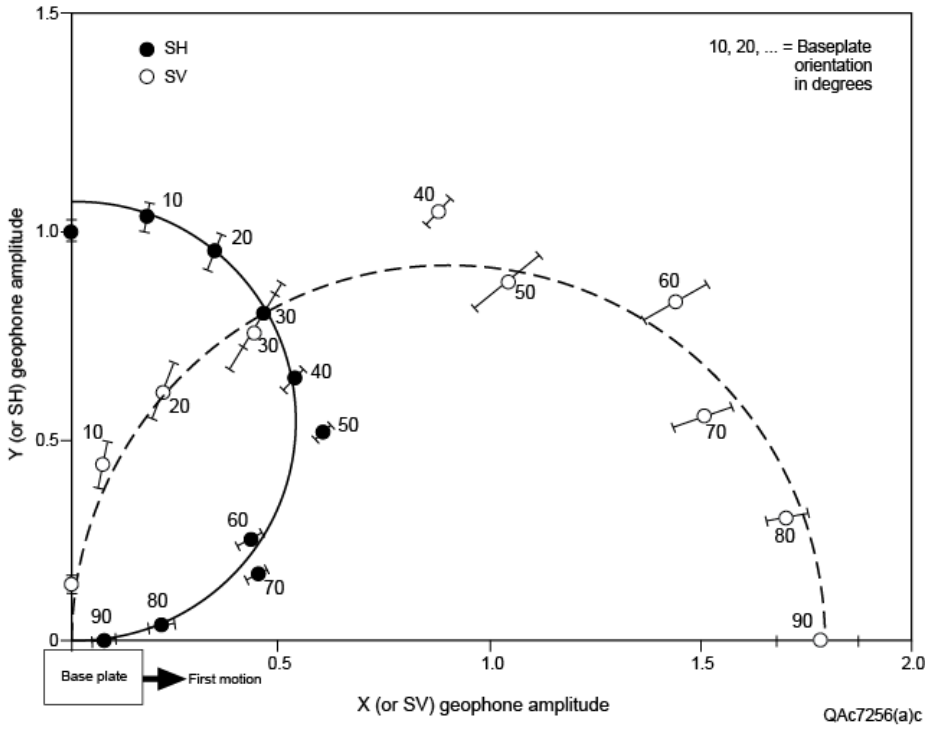

Fig. 13. Radial-S and transverse-S radiation patterns published by Robertson and Corrigan (1983).

There are strong similarities in the radiation patterns exhibited in these two figures. In each test, radial-S and transverse-S modes spread away from the source station in orthogonal directions, and radial-S energy is stronger than transverse-S energy. In our analysis (Fig. 12c), the ratio of radial-S to transverse-S energy is higher than what Robertson and Corrigan observed (Fig. 13). We made no attempt to calibrate the responses of the two horizontal geophones in our test so we do not know if equal impulses on our radial and transverse geophones produce equivalent outputs. If the radial and transverse geophones produce data with different amplitude strengths, the radial-S and transverse-S amplitudes plotted on Fig. 12c could be biased. Neither did we attempt to determine if our wall-locked radial and transverse geophones were equally coupled to the formation. In the test conducted by Robertson and Corrigan (1983), their downhole geophone was cemented in place and probably had excellent coupling of all three sensing elements. Perhaps most importantly,

we did not verify that the base plate of the horizontal vibrator was uniformly coupled to the earth at each vehicle orientation so that a constant horizontal force was generated in each azimuth direction. For two base-plate orientations (40° and 70°), there was an unexplained increase in amplitude on radial and transverse geophones. We assumed these anomalous amplitudes were caused by a different base-plate coupling for these vibrator orientations. We had to decide whether to delete the data for these two base-plate orientations or to apply a scaling factor that forced the data into the range of the companion data observed for all other base-plate positions. We elected to scale the data so that trace amplitudes agreed with the amplitude trends observed for the family of traces exhibited on Figs. 12a and 12b. The resulting positions of the 40° and 70° azimuth data points on Fig. 12c appear reasonable but could be eliminated without altering the transverse-S and radial-S radiation patterns that are shown.

One difference in the two test sites represented by the data exhibited on Figs. 12 and 13 is that Robertson and Corrigan positioned a single 3C geophone at a shallow depth of 430 ft (131 m) in a reasonably uniform shale layer; whereas, our receiver was 1386 ft (422 m) deep in stratified layering (Fig. 2). Our measurement may be more representative of the attributes of radial-S and transverse-S modes that propagate in layered media. Robertson and Corrigan recorded several individual vibrator sweeps at each base-plate orientation and established error bars on their measurements presented as Fig. 13. In contrast, we summed two vibrator sweeps at each base-plate orientation and did not repeat measurements at any vehicle orientation. Thus we show no error bars on our data.

CONCLUSIONS

The analysis of VSP test data acquired at the Devine Test Site confirmed that direct-S modes are produced by vertical vibrators and suggests these modes can be substituted for direct-S modes produced by horizontal vibrators in some instances. An appealing aspect of direct-S modes produced by vertical vibrators is that they have a higher range of frequencies than do direct-S modes produced by horizontal vibrators, and thus vertical vibrator direct-S [illegible]

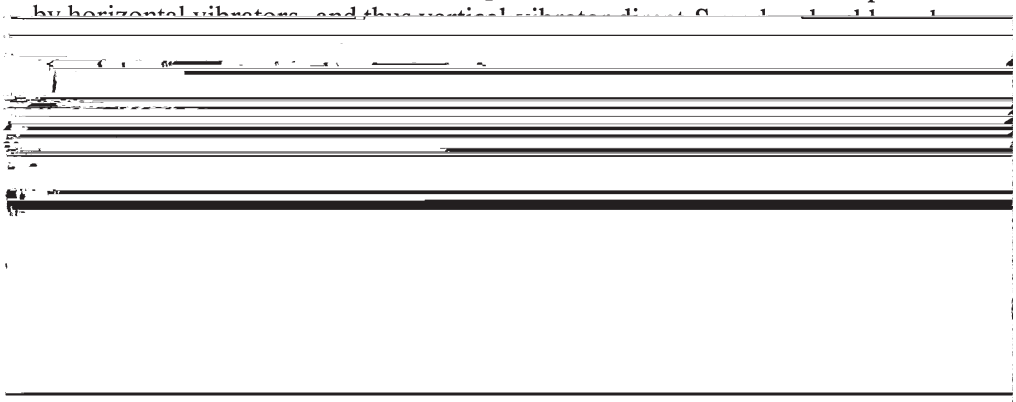

analyses of direct-S wave modes generated by all types of vertical-force sources deployed in different array geometries and compare these results with direct-S radiation generated by horizontal-force sources.

This research is significant because one implication is that direct-S data acquisition can be done in some instances with only vertical vibrator sources without the necessity of deploying horizontal vibrators. Because vertical vibrators are widespread but horizontal vibrators are not, a second implication is that direct-S data acquisition can be considered across many areas where S-wave technology may otherwise not be done. These research results thus impact seismic imaging technology, the fundamental theme of this journal.

Perhaps the most important consideration is that the cost of acquiring multicomponent seismic data can be reduced by using vertical-force sources to generate direct-S waves. Because of the potential commercial value of using vertical-force sources to generate direct-S modes, the concepts illustrated in this paper have been patented by the Board of Regents of The University of Texas System (Hardage, 2011).

ACKNOWLEDGMENTS

These source tests could not have been done without the assistance of sponsors of the Exploration Geophysics Laboratory. Mitcham Industries provided the MaxiWave system used for the vertical array as well as surface 3C geophones and DSU3 sensors, a recording truck, and field technicians. Halliburton provided wireline services and engineers, Dawson Geophysical provided vibrators, vibrator support personnel, and transportation for other sources, Sercel provided a 428 recorder, support personnel, and Unite cable-free boxes. Seismic Source and i-Seis combined to provide Sigma cable-free boxes, a Universal Encorder, and engineering staff. Austin Powder provided explosives and a certified shooter. United Services Alliance and Vecta Technology provided their accelerated-weight (nitrogen-spring) source and source operators. OyoGeospace provided a variety of special geophones, GSR cable-free boxes, and field personnel.

REFERENCES

DiSiena, J.P., Gaiser, J.E. and Corrigan, D., 1981. Three-component vertical seismic profiles - orientation for shear wave analysis. Expanded Abstr., 51st Ann. Internat. SEG Mtg., Los Angeles, Paper S5.4, 1990-2011.

Edelmann, H.A.K., 1981. Shover shear-wave generation by vibration orthogonal to the polarization. Geophys. Prospect., 29: 541-549.

Fertig, J., 1984. Shear waves by an explosive point-source - the earth surface as a generator of converted P-S waves. Geophys. Prosp., 32, 1-17.

Fertig, J. and Krajewski, P., 1989. Acquisition and processing of pure and converted shear waves generated by compressional wave sources. Surv. Geophys., 10: 103-132.

Hardage, B.A., 2000. Vertical Seismic Profiling - Principles. Third updated and revised ed., Pergamon Press, 552 pp. (Eds. 1 and 2 published in 1983 and 1985 by Geophysical Press, Amsterdam).

Hardage, B.A., 2009. Horizontal wave testing. AAPG Explorer, 30 (12): 26-27.

Hardage, B.A., 2010. Vertical wave testing. AAPG Explorer, 31 (1): 32-33.

Hardage, B.A., 2011. System and method for acquisition and processing of elastic wavefield data. U.S. Patent 8,040,754 B1.

Li, X.Y., MacBeth, C. and Crampin, S., 1998. Interpreting non-orthogonal split shear waves for seismic anisotropy in multicomponent VSPs. Geophys. Prosp., 46: 1-27.

Lynn, H.B. and McCardle, M., 1990. Four 3-component VSPs from South Texas onshore - S-wave velocities for AVO and discussion of acquisition parameters. Expanded Abstr., 60th Ann. Internat. SEG Mtg., San Francisco, BG3.2, 9: 52-55.

Miller, G. and Pursey, H., 1954. The field and radiation impedance of mechanical vibrators on the